Supporting Information:

Sweep, Step, Pulse, and Frequency-Based Techniques Applied to Protein Monolayer Electrochemistry at Nanoparticle Interfaces.

Debbie S. Campbell-Rance, Tran. T. Doan and Michael C. Leopold*
Department of Chemistry, Gottwald Center for the Sciences, University of Richmond
Richmond, VA 23173

Contents:

* To whom correspondence should be addressed. Email: mleopold@richmond.edu. Phone: (804) 287-6329. Fax: (804) 287-1897.

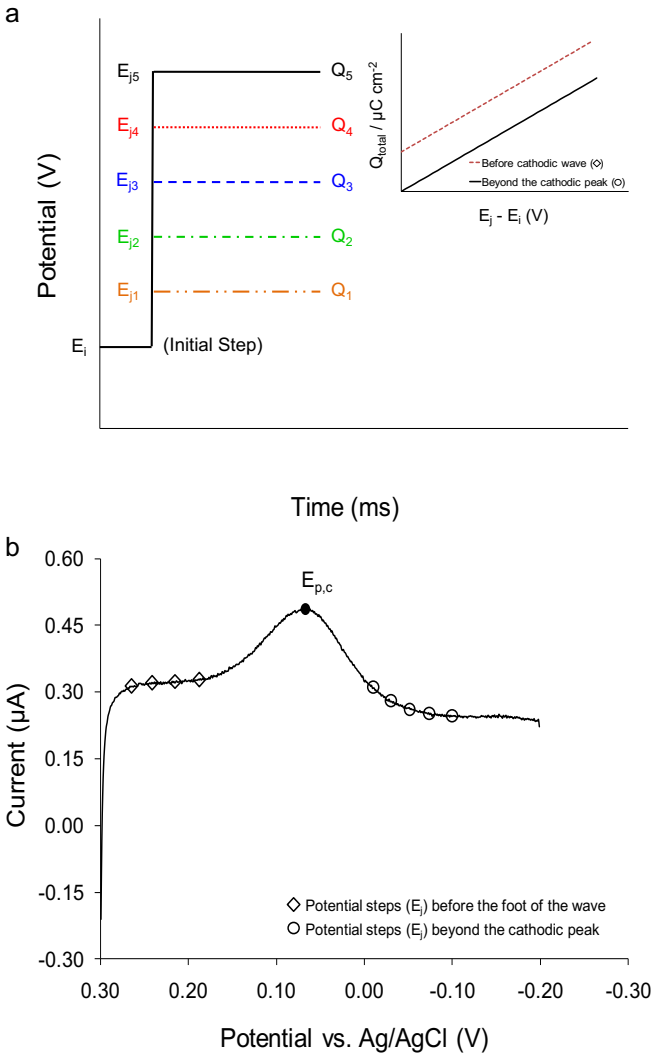

Fig. S1. Waveform applied during chronocoulometry (CC) experiments on PME systems where the potential is stepped from an initial value (E_i) to potentials (E_{j1}, E_{j2}…) before and after the reduction potential of the adsorbed protein (e.g. $E_{p,c\ (AZ)}$ = 82 mV) while the corresponding charge (Q) is measured and plotted vs. potential (E_j - E_i) to show the theoretical linear relationship of Eq. (5) (Inset); (b) Linear sweep voltammogram reduction wave for AZ at a 5 layer MPC film and illustrating the potential steps positive/before (E_j = 0.275 to 0.200) and negative/after (E_j = -0.065 to -0.225) the protein cathodic peak potential ($E_{p,c}$).

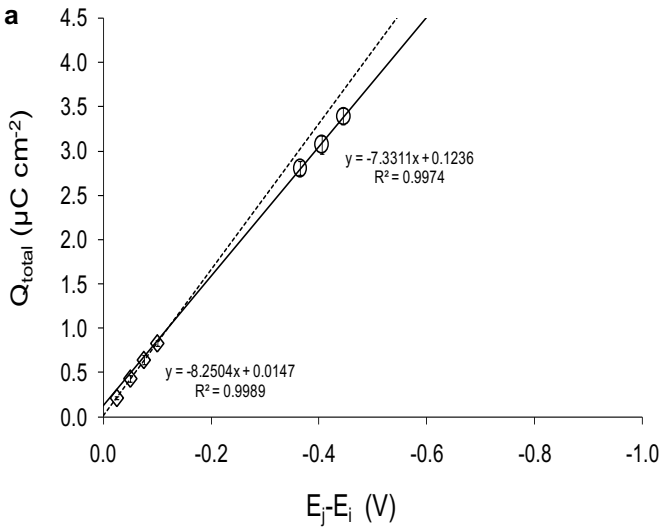

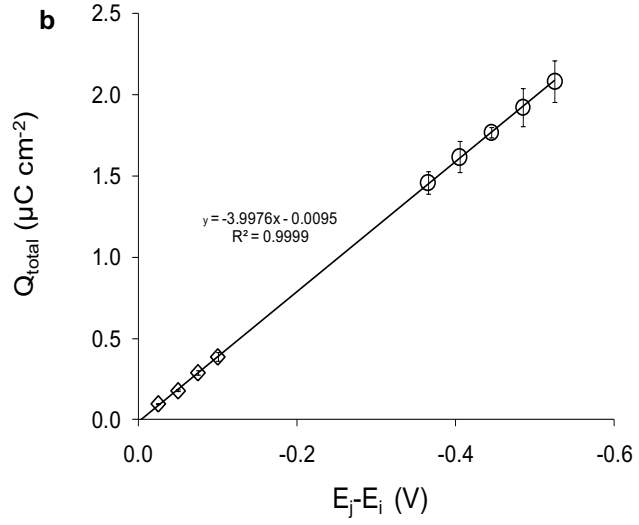

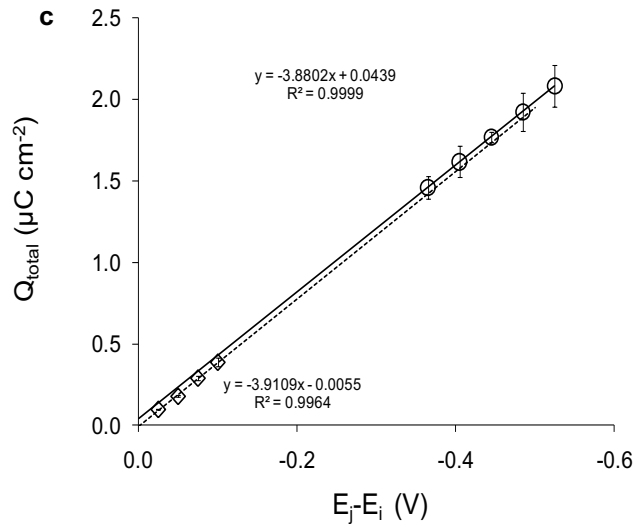

Fig. S2. Chronocoulometry (CC) results for MPC film assemblies in 4.4 mM potassium phosphate buffer (pH = 7.0, μ = 10 mM). (a) Data for $(MPC)_3$ / C6 SAM / Au with no AZ adsorbed (control) plotted with two separate regression analyses for steps before and after $E_{p,c}$; Chronocoulometry results for $(MPC)_3$ / C6 SAM / Au with charge passed from potential steps before $E_{p,a}$ (from E_i = -200 mV to E_j = -175 to -100 mV), marked as (◊) and those after $E_{p,a}$ (from E_i = -150 mV to E_j = 150 to 250 mV) marked as (○) plotted as either (b) a single regression analysis or (c) separate regression analysis for each set of steps. Note: n = 5, the number of replicate measurements.

Table S1
Tracking the estimations of C_{dl} (CC slope) as a function of potential steps direction during CC

	C_{dl} (μF cm^{-2}) or Slope			
	Reductive Potential Steps		*Oxidative Potential Steps*	
Platform	Before $E_{p,c}$	After $E_{p,c}$	Before $E_{p,a}$	After $E_{p,a}$
Self-Assembled Monolayers				
C6 SAM / Au	3.22 ± 0.45	3.17 ± 0.02	N/A	N/A
AZ / C6 SAM / Au	3.18 ± 0.49	3.09 ± 0.02	N/A	N/A
MPC Film Assemblies				
$(C6\ MPC)_3$ / SAM / Au	8.25 ± 0.20	7.33 ± 0.37	3.91 ± 0.17	3.88 ± 0.03
AZ/$(C6\ MPC)_3$ /SAM/Au	7.22 ± 0.06	5.11 ± 0.05	3.45 ± 0.19	4.24 ± 0.05

Note: n = 4, number of replicate measurements involved in data acquisition

1. Alternate Azurin Purification to Check Homogeneity of Protein Population

In addition to the standard purification procedure cited in the experimental section two other purification procedures were attempted to assess the homogeneity of the AZ protein used in this study. Both purification procedures used AZ that had been initially prepared and purified according to the protocol described by Vargo et al [1]. The first purification procedure was an ion-exchange separation modeled after the procedures used to purify cyt *c* [2]. Briefly, the carboxymethyl cellulose packed (CM-52 Whatman) column was hydrated with a 40 mM potassium phosphate buffer (KPB, pH = 7.0, μ = 90 mM)) prior to the loading of AZ. AZ in 4.4 mM KPB (pH = 7.0, μ = 10 mM) was subsequently passed through the column with eluting solvent 70 mM KPB (pH = 7.0, μ = 160 mM). The AZ fraction was collected and concentrated using an Amicon filtration system (YM-10 membrane). The second purification procedure utilized a smaller size exclusion column packed with Sephadex G-25 that was first equilibrated with 4.4 mM KPB. Once the AZ sample had been loaded on this column, it was then eluted from the column with continuous addition of the buffer. The protein was collected, its concentration checked with UV-Vis spectroscopy, and its purity (homogeneity) checked with gel electrophoresis as described below.

2. SDS PAGE Analysis

SDS PAGE gel electrophoresis was used to probe the different purification procedures for evidence of multiple protein populations in the AZ samples. The SDS page result for AZ separation using CM-52 Whatman column and Sephadex G-25 column are displayed in Fig. S1a and S1b, respectively. In both cases, AZ samples from these purification attempts were simultaneously analyzed and compared to AZ stock samples (prepared and purified according to Vargo et al.) using SDS PAGE under reducing and now reducing conditions. As seen in Fig. S1a and S1b the band in the first lane of both SDS PAGE results represents the standard. Identical protein bands are observed in the SDS PAGE analysis comparing AZ separated on CM-52 Whatman column and AZ from the stock, both under reducing and non-reducing conditions. This result suggests that AZ separation was not improved using the CM-52 Whatman column. The SDS PAGE result for AZ separated on the Sephadex G-25 column was indistinguishable from that of AZ stock under reducing conditions. In contrast, some of the bands present under non-reducing condition for AZ separated on the Sephadex G-25 column were absent in AZ stock solution as see in Fig. S1b. This suggests that AZ separation on the Sephadex G-25 column has shown improved homogeneity in protein population compared to protocol reported by Vargo et al[1].

a

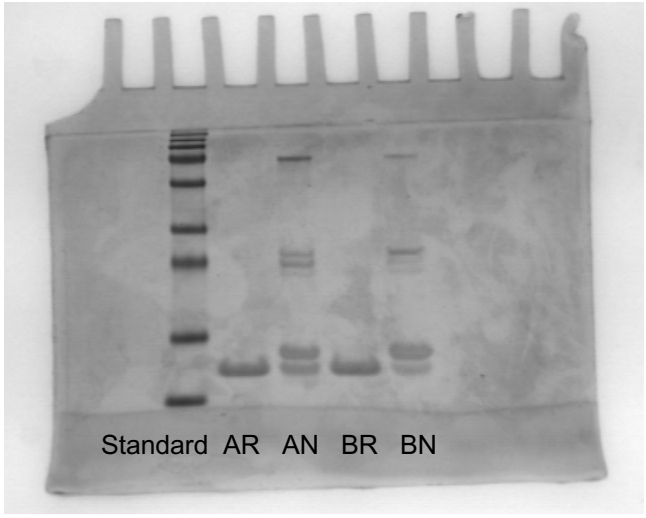

b

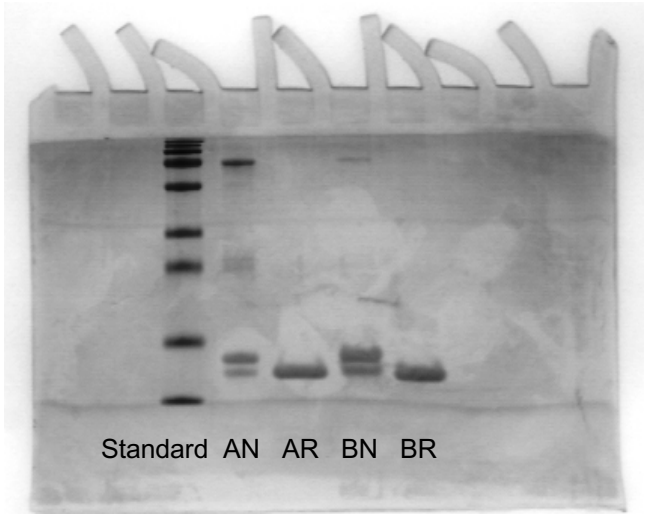

Fig. S3. Sodium dodecyl sulfate polyacrylamide gel electrophoretic (SDS PAGE) analysis of AZ after purification attempts . (a) SDS PAGE of AZ purified on column (25 cm x 1 cm) packed with carboxymethyl cellulose, (CM-52 Whatman) (AR and AN) and AZ stock solution (BR and BN). (b) SDS PAGE of AZ purified column (12 cm x 2 cm) packed with Sephadex G-25 (AN and AR) and AZ stock solution (BN and BR). In each case AR and BR refer to reducing conditions and AN and BN refer to non-reducing conditions. The stock samples of AZ (BR and BN) are samples prepared and purified using protocol reported by Vargo et al.

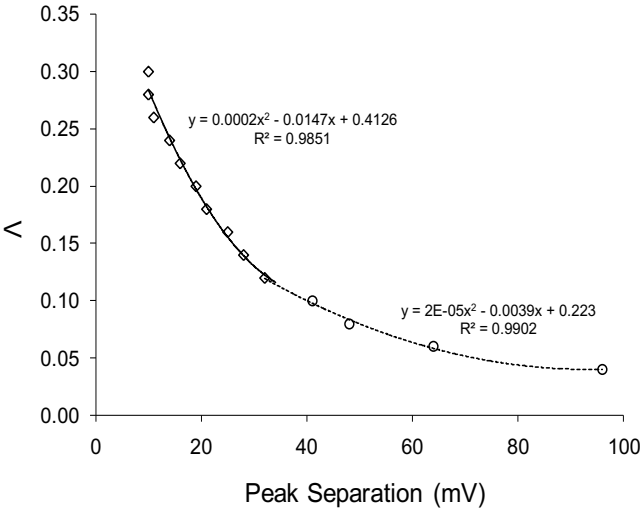

Fig. S4. Working curve generated from SWV simulations (DigiElch) with peak separation (ΔE_p) ≥ 10 mV after changing ΔE from 4 to 16 mV. The quadratic equation used to fit the portion of the working curve having ΔE_p > 40 mV was used to estimate Λ from square wave voltammograms of AZ / C12 $(MPC)_3$ / C14 SAM / Au with ΔE_p > 40 mV . The trendline with diamond markers was generated from simulated voltammograms with 10 ≤ ΔE_p ≤ 40 mV whereas the trendline with circular markers was generated from simulated voltammograms with ΔE_p > 40 mV.

3. Electrochemical Impedance Spectroscopy Theory

Cole-Cole plots are a direct manipulation of the Nyquist (Bode) plot where the total impedance of the system is given by the following equation:

$$Z = Z_{Re} - jZ_{Im} \tag{S1}$$

The x-axis (real part) in the Cole-Cole plot is:

$$\mathrm{Re}\left[\frac{1}{j\omega Z}\right] = \frac{Z_{Im}}{\omega}\left(Z_{Re}^2 + Z_{Im}^2\right) \tag{S2}$$

and the y-axis is:

$$-\mathrm{Im}\left[\frac{1}{j\omega Z}\right] = \frac{Z_{Re}}{\omega}\left(Z_{Re}^2 + Z_{Im}^2\right) \tag{S3}$$

where $j = (-1)^{1/2}$, $\omega = 2\pi f$ and f is the frequency. The shape of a typical Cole-Cole plot is a semicircle which is affixed to the origin on real axis, $\mathrm{Re}[1/j\omega Z]$, and its diameter is C_{dl} or $(C_{dl} + C_{AD})$ in the absence or presence of the redox species, respectively [11, 66, 67].

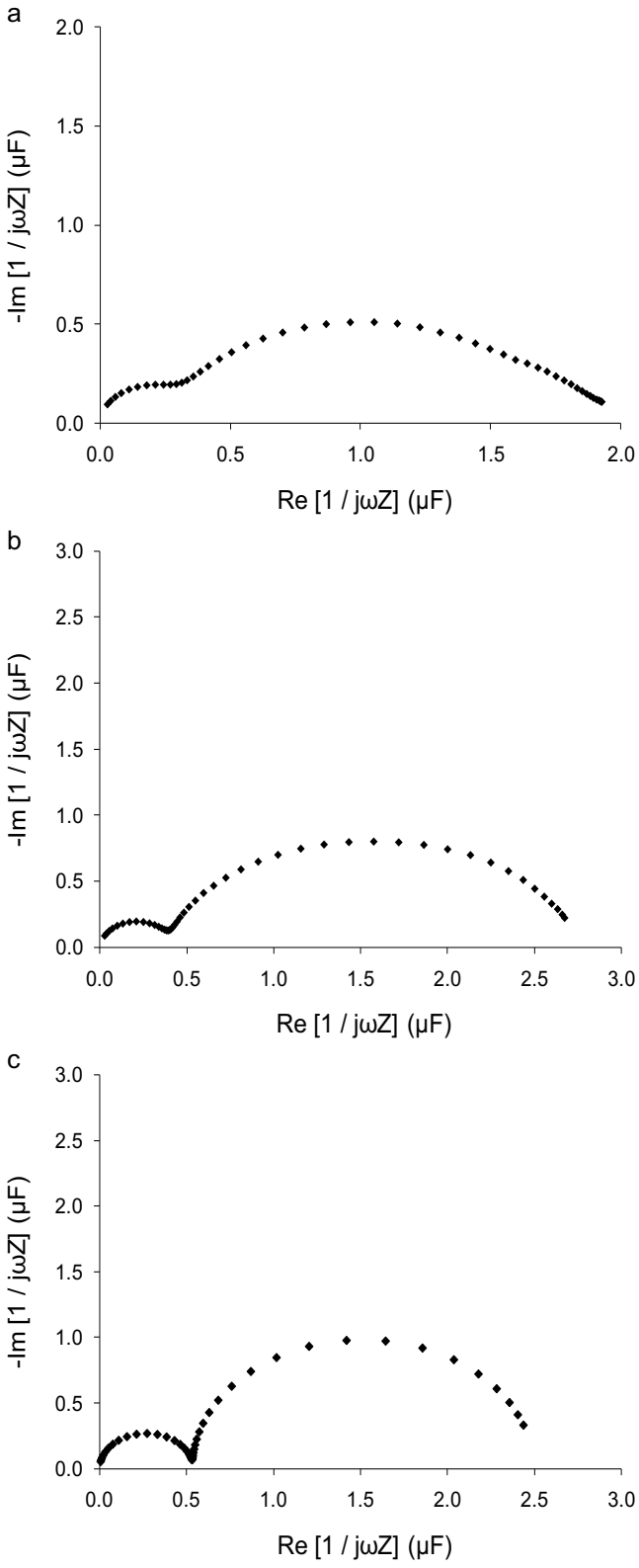

Fig. S5. Cole-Cole Plots of AZ adsorbed on gold electrode modified with alkanethiols of varying chain lengths: (a) AZ / C18 SAM / Au, (b) AZ / C16 SAM / Au and (c) AZ / C14 SAM / Au in 4.4 potassium phosphate buffer (pH = 7.0, μ = 10 mM). The small high frequency semicircle (left) which represents the non-Faradaic charging of the double layer becomes more distinct the greater the number of methylene units in the chain.

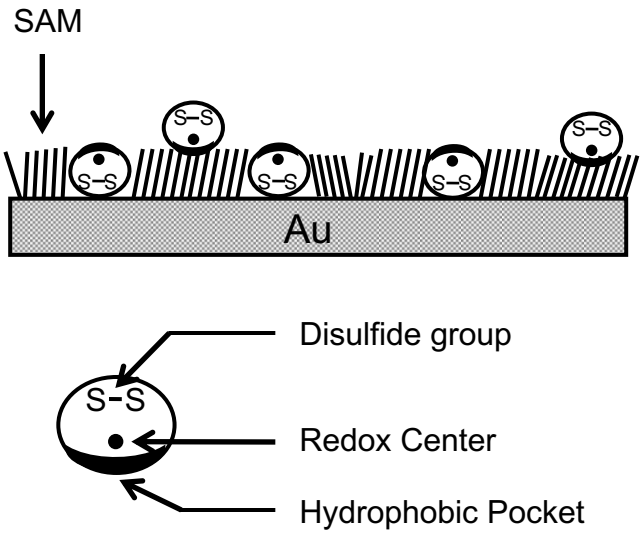

Fig. S6. Possible orientations of AZ on C6 SAM modified Au substrate. The greater defect density of the C6 SAM makes it possible for AZ to bind via the hydrophobic pockets near the copper redox center or directly on the gold substrate through the disulfide bonds from the cysteine residue on the opposite side of the protein. AZ having dual orientations on the SAM platform could impact the measured rate constant (k_{et}).

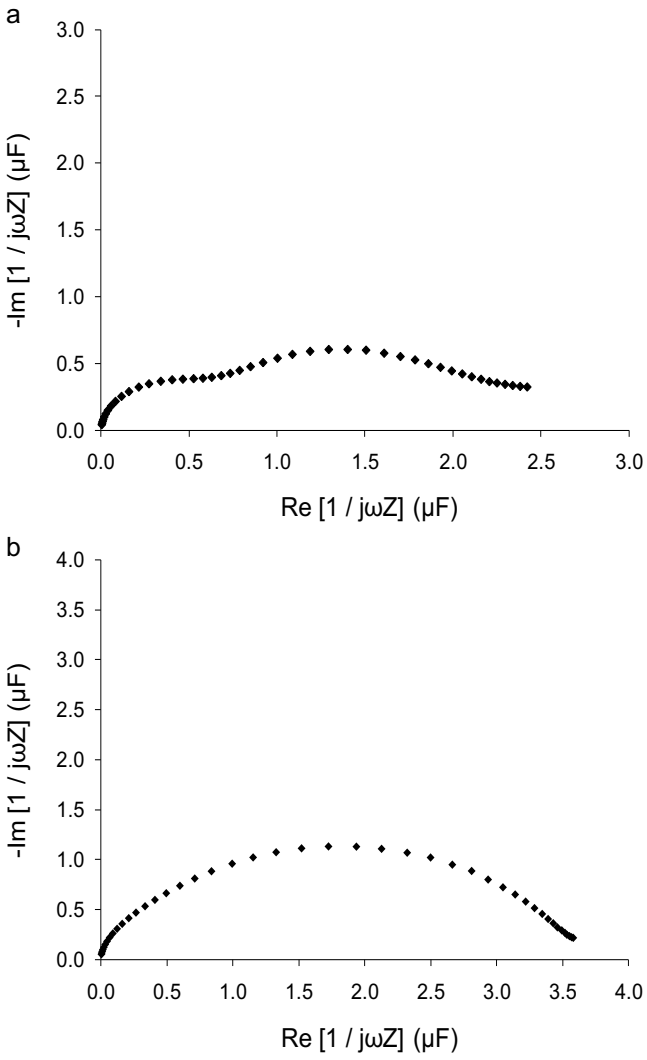

Fig. S7. Cole-Cole Plots of (a) unpurified (as received) and (b) purified (CM-52, Whatman) cyt *c* adsorbed at 11-mercaptoundecanoic acid SAM modified gold electrodes, showing multiple population of protein present in the unpurified sample.

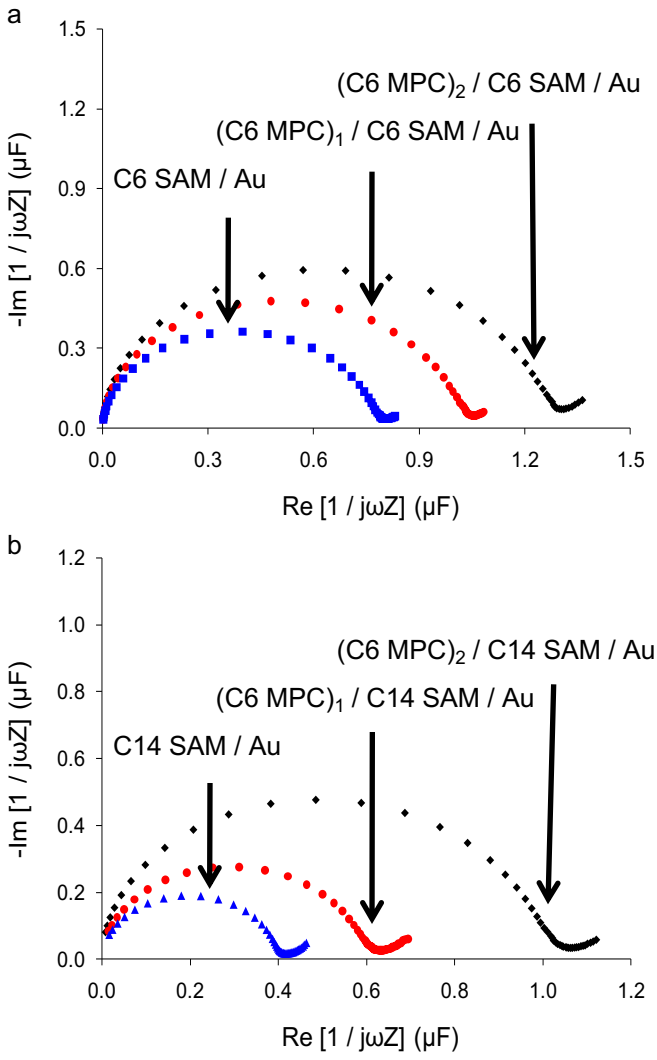

Fig. S7. Impedance spectra (Cole-Cole) tracking the growth of C6 MPC film assembly on gold substrate. (a) Growth of 2 layers of 1, 9-NDT linked C6 MPCs on C6 SAM. (b) Growth of 2 layer of 1, 9-NDT linked C6 MPC on C14 SAM.

Table S2
Tracking the growth of C6 MPC film assembly on C6 and C14 modified gold substrate via C_{dl} values.

	C_{dl} (μF cm^{-2})		
Platform	CV	EIS (CNLS)	EIS (Cole –Cole)
C6 SAM / Au	3.09 ± 0.02	2.90 ± 0.01	2.95 ± 0.04
$(C6\ MPC)_1$ / C6 SAM / Au	3.60 ± 0.13	3.64 ± 0.26	3.63 ± 0.18
$(C6\ MPC)_2$ / C6 SAM / Au	4.39 ± 0.40	4.57 ± 0.41	4.49 ± 0.43
C14 SAM / Au	1.57 ± 0.04	1.49 ± 0.04	1.48 ± 0.02
$(C6\ MPC)_1$ / C14 SAM / Au	2.58 ± 0.31	2.47 ± 0.19	2.43 ± 0.22
$(C6\ MPC)_2$ / C14 SAM / Au	3.45 ± 0.25	3.43 ± 0.26	3.43 ± 0.28

Note: n = 4, number of replicate measurements involved in data acquisition

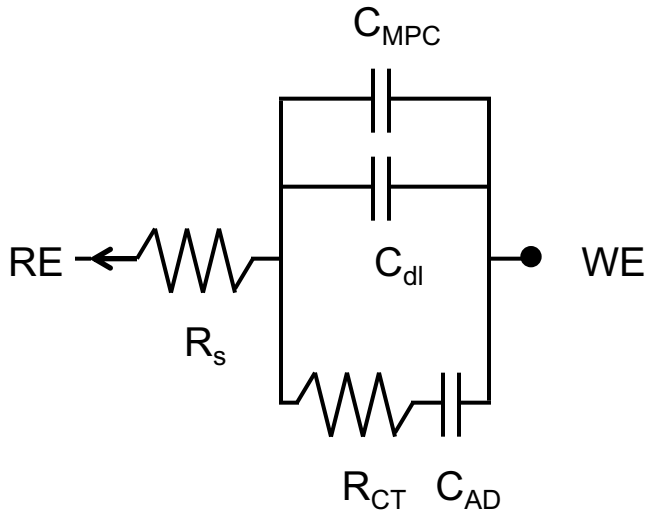

Fig. S8. Based on the capacitive behavior of MPCs, a modification to the Randles equivalent circuit is proposed which characterizes the behavior of surface adsorbed species at such an interface [69, 70]. The circuit involves the addition of an extra capacitor in parallel with the double layer capacitor of the film to represent the added capacitance from the incorporated MPCs. We note, however, that this parallel capacitor is merely symbolic/visual as it is just another contributing factor to the overall capacitance and that the circuitry is essentially unchanged.

Additional References

[1] M. L. Vargo, C. P. Gulka, J. K. Gerig, C. M. Manieri, J. D. Dattlebaum, C. B. Marks, N. T. Lawrence, M. L. Trawick, and M. C. Leopold, Langmuir 26:560 (2010).

[2] A. F. Loftus, K. P. Reighard, S. A. Kapourales, and M. C. Leopold, Journal of the American Chemical Society 130:1649 (2008).